

Thermal management of using crystallization-controllable supercooled PCM in space heating applications for different heating profiles in the UK

Cagri Kutlu^{a,*}, Yuehong Su^a, Qinghua Lyu^b, Saffa Riffat^a

^a Department of Architecture and Built Environment, University of Nottingham, University Park, NG7 2RD, UK

^b School of Science, Hubei University of Technology, Hubei, Wuhan, China

ARTICLE INFO

Keywords:

Controlled crystallization
Heating profiles
Sodium acetate trihydrate
Thermal management

ABSTRACT

Supercooled sodium acetate trihydrate (SAT) allows the latent heat can be released when it is externally triggered regardless of the supercooling degree. Thus, the implementation of SAT into heating systems can eliminate the negative effects of weather variation and increase the utilization of solar energy by storing the heat for days. However, supercooled PCMs can lose a serious amount of latent heat when their temperature falls to ambient temperature. Moreover, the poor heat conductivity of the SAT can cause providing insufficient temperature in the houses for different heating profiles which require auxiliary heating. In this study, the dynamic thermal behaviour of a supercooled PCM-immersed storage tank for heating different dwellings is investigated based on different activation orders of the PCM tubes. The controlled PCM activation order shows that the hot water supply temperature can be increased compared to the activation of all tubes at midnight. Controlled triggering resulted in performance improvement in all heating profiles by an increment of 1.5 °C, but it is more promising for the Eco-house heating profile as it reaches 4.3 °C. Moreover, this method reduces the daily heat loss from the PCM storage tank by up to 1.3 kWh. It is also found that the PCM loses its 35% of latent energy after three days of storage.

1. Introduction

Nowadays, integration of renewable energies on the building systems is an important need as the energy consumption in the buildings is considered as an increasing proportion of total energy consumption around the world [1], and it has been reported that 32.5% of the UK energy usage is consumed by buildings [2]. In the renewable energy integrated building applications, one of the important issues is providing heating on building demand because; intermittency, mismatch between demand and supplying energy timing and varying ambient conditions make using solar energy in building a cumbersome. Therefore, thermal energy storage (TES) systems have been offered to ensure sustainable heat supply [3,4]. Although using latent heat storage systems are the cheapest and convenient for short term heat storage [5], for medium to long term heat storage periods, latent heat systems continue to loss heat even they are not in use, thus the heat is wasted.

Controllable crystallization of the phase change material (PCM) can be a solution to this heat waste. The supercooled feature allows that the latent heat is only released when triggered to induce crystallization, even when stored at ambient temperature. While supercooling is

generally considered a significant disadvantage in conventional PCM heat storage systems, in this system it turns the problem into an asset by controlled activation. Several supercooled materials' properties and triggering methods have been investigated and tested by many researchers and the most well-known is supercooled sodium acetate trihydrate (SAT). Its melting point is 58 °C and the latent heat of crystallization is 247 kJ/kg in a certain concentration level where the melting temperature depends on salt-water concentration. The heat is released by activating the triggering device and exothermic crystallization allowing temperatures of 58 °C to be reached in minutes [6]. Incorporation of these materials with heat pump units can promote the system. Since gas boilers release high CO₂ to the environment, heat pump usage has been recommended to the public by the governments for space heating and hot water purposes in buildings. However, the current UK daily national grid reaches peak value in the evening around 17:00–18:00 and it was informed that the heat pump load profile reaches a peak in the morning around 07:00–08:00 with 20% of the contribution to the morning peak. It means the morning peak would be higher in the future with higher developments of the heat pumps [7]. Thus, it is important to find a way to both cover environmental issues

* Corresponding author.

E-mail address: cagri.kutlu2@nottingham.ac.uk (C. Kutlu).

<https://doi.org/10.1016/j.renene.2023.02.077>

Received 16 November 2022; Received in revised form 22 January 2023; Accepted 17 February 2023

Available online 19 February 2023

0960-1481/© 2023 The Authors. Published by Elsevier Ltd. This is an open access article under the CC BY license (<http://creativecommons.org/licenses/by/4.0/>).

like using heat pumps and also consider the grid load. Load shifting with thermal storage is getting popular in heating applications as it also allows solar energy utilization. Teamah et al. [8] showed that a ground source heat pump with PCM-enhanced thermal storage can successfully provide load shifting. Xu et al. [9] presented that when the daytime charging strategy is applied for space heating by heat pumps, indirect CO₂ emissions can be reduced by up to 14% compared to the off-peak charging strategy. However, this short-term load shifting may not work very well if solar energy is the main heat source for the heat pump. Supercooled PCM can be effectively used for variable solar profiles as it can allow storage solar assisted heat pump's heat even for a week period at room temperature and still having some proportion of the latent heat [10]. Moreover, in order to increase the effectiveness of PCM usage in heat storage systems, controllable heat discharge can be key for more efficient systems because performance of using PCM in water tanks is dependent on the operating conditions [11]. Therefore, the attention on controlled triggering increases for even different supercooled PCM materials such as erythritol for higher temperature applications [12].

Regarding space heating and DHW applications, some techniques to trigger the crystallization of supercooled SAT have been published such as inserting SAT crystals [13], local cooling by cold touch [14] or using a Peltier device [15], percussion vibration [16] and they were used in some applications successfully. However, studies on electric nucleation are not enough in the literature to conclude its effectiveness, thus, successful nucleation by electrical triggering is accepted as uncertain [17]. Recently, Dong et al. [18] presented electrically-controlled crystallization of supercooled SAT solution techniques which allows to release heat from the supercooled SAT solution. Chen et al. [19] carried out lab-scale tests of SAT and prepared a composite mixture to increase the thermal conductivity. They maintained stable supercooling for electrically-triggered nucleation.

Application of supercooled SAT as a heat storage in the heating systems have been investigated but limited. Dannemand et al. [14] experimentally tested two SAT units at laboratory and measured discharged energies after repeating tests. They used liquid CO₂ to cool surface of the container to initiate nucleation. Englmair et al. [6] prepared an experiment for a solar combi-system using SAT. Tubular collectors and segmented PCM heat storage prototype were used and different control strategies was tested for enabling the best automated system operation. Kutlu et al. [20] carried out a simulation study by using controllable crystallization of SAT for domestic hot water application to eliminate morning peak. The PCMs were activated in the early morning to prepare hot water, they informed that daily energy consumption can be reduced around 13% in an average solar day. Englmair et al. [21] investigated on-demand crystallization of SAT in solar combi system, they calculated that annual solar fraction of 71% can be achieved by using 22.4 m² collector area and 1 m³ PCM storage in a Danish passive house. Recently, Kutlu et al. [10] carried out a simulation study of a solar-assisted heat pump unit with controllable SAT to provide space heating to a building. They presented that PCM storage tank can be charged in 6.5 h and the stored tank can provide one-day heating, which will promote solar assisted heat pump instead of an air source heat pump.

As seen from the literature, controllable crystallization of SAT is a promising method for load shifting and utilization of renewable energy in heating applications. Its ability to control heat release makes it suitable for demand-based heating systems which have been still in progress by using conventional PCM applications. However, the number of studies about the controllable crystallization of SAT is limited and its adaptation to building applications should be further investigated to show its potential. For this purpose, this study proposes a different perspective for the controllable crystallization of SAT applications. Apart from activating heat release at one time in a day, this study offers partial activation of charged PCM tubes according to peak heating demand periods. In this way, daily heat loss from the storage tank can be reduced and the supply water temperature to the building will be higher.

Based on these targets, an electrical triggering device has been prepared to trigger the crystallization inside the stainless-steel tube. After proving the controlled heat release, the concept of controllable crystallization of SAT will be further investigated especially considering the performance of heating supply to the buildings for different profiles. Therefore, the ability of the supercooled PCM storage tank to provide heating to different UK heating profiles is investigated in this study. Moreover, the effect of the initial temperature should be examined because storage time affects the latent heat capacity after activation of the SAT. Thus, a strategy is developed to have the advantage of different activation times. With this application, the hot water supply temperature can be increased at the end of the day and heat loss can be reduced.

2. Heat pump heating profiles of the buildings in the UK

As the proposed study presents the ability to heat for different profiles in the UK, monitored real data for heat pump systems were used. Heat pump heating profiles were taken from the datasets of the Renewable Heat Premium Payment (RHPP) trial [22]. The RHPP scheme was administered by the UK Energy Savings Trust and Buildings Research Establishment to run the meter installation and data collection phases of the monitoring program. The data was collected from October 31, 2013 to March 31, 2015 which is based on monitored around 700 UK homes. The data is both domestic hot water and space heating and was recorded at a 2-min resolution. The data shows the general heat pump trend in the UK as it covers many different indicators affecting on heating profile. Such as, consumer control strategies were observed in widespread patterns of thermostat set points which ranged between 18 °C and 23 °C. The work also covers different locations in the UK, weather conditions have an effect on the results in addition to building age and fabrics. In order to regroup these parameters, the heating profiles have been generated by clustering all houses that match the given combination [23]. The dataset includes metadata describing the kind of heat pump, the tenure and the type of dwelling of each site. Details of the classified buildings are given in Table 1.

Although ground-source heat pump (GSHP) and air-source heat pumps (ASHP) are used in the classified buildings, the heating demand from the building is assumed as same regardless of heat pump type. Emitter types are also combination of radiators and underfloor heating, and property age shows the variety of the insulation and fabric of the buildings. Therefore, Fig. 1 shows the average hourly heating demands of classified buildings. Group 3 has three bedrooms; the rest have four or more bedrooms. Considering daily average heating demands, Groups 1 to 3 are around 30 kWh, however, Group 4 and Group 5 are around 50 kWh daily heating demands. The reason for this, of course, the sizes, ages and types of houses even the locations are different, but the figure gives us information about heating profiles and trends. It is necessary to test the proposed supercooled PCM system's heating supply performance regarding given profiles which is the objective of this study.

To show the ability of the heating supply for the buildings, two different heating trends were chosen to compare. Since Group 2 shows a more stable heating requirement with a morning peak, and Group 5 shows two-peak heating times in a day, these profiles are chosen to represent different heating profiles. Undoubtedly, daily heating requirements are different for these groups, so normalizing was carried out for Group 5. In this way, the daily heating demand of Group 5 is reduced

Table 1
Classified buildings in the study.

Group	HP Type	Property Type	Property Age	Emitter Type
Group 1	GSHP	Detached	After 2000	Underfloor
Group 2	ASHP	Detached	Pre 1919	Radiator
Group 3	ASHP	Detached	1965–1980	Underfloor
Group 4	GSHP	Detached	Pre 1919	Both
Group 5	GSHP	Semi-Detached	Pre 1919	Both

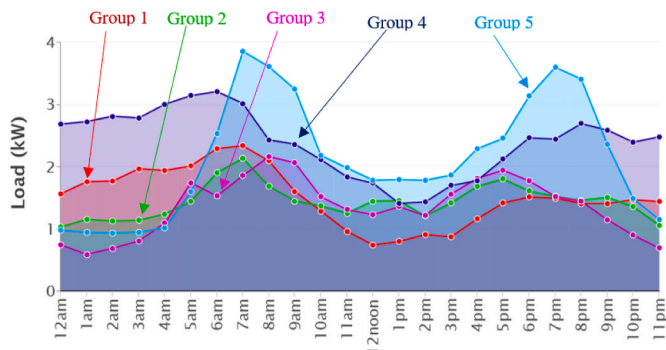


Fig. 1. Average heating demands of classified buildings.

to 30 kWh from 50 kWh by multiplying the hourly demands while keeping the trend the same. In this way, same size of PCM storage tank can be tested in simulation because geometry and size of the storage tank has an influence on heating supply performance.

On the other hand, these houses are conventional houses in the UK, but the number of eco-houses or low-carbon houses has increased over the world to reduce heating costs and CO₂ emissions, thus, to extend the impact and range of the study, the data from our previous study [10] has been used in order to show another heating profile. In the previous study, one of the Creative Energy Homes at the University of Nottingham on Park Campus a low-carbon building, The David Wilson Millennium Eco-house was simulated [24]. This house was built to support domestic size renewable energy systems. Thus, it uses air conditioning standards to provide thermal comfort to residents. The IESVE model [25] was used with real Nottingham, UK yearly weather data. The house is a two-story office building with dimensions of 7.9 m × 7.9 m × 5.0 m with interior floor area of 62.41 m² for each floor. It is assumed that a family of 4 people live in the house. The main construction elements and U-values of the house were taken as: External wall 0.22 W/(m²K), roof 0.19 W/(m²K), glazing 1.8 W/(m²K), door 2.2 W/(m²K) and floor 0.2 W/(m²K). Natural ventilation is 5 l/s/person, and infiltration rate is taken as 0.3 ach. The temperature setting is 18 °C from 22:00 to 05:30, 15 °C during unoccupied hours (7:30 to 18:00) and 21 °C during the remaining times.

The used envelope, people profile and ventilation systems have an effect on the building heating demand profile. The heating rate will always decrease over time in conventional PCM storage systems because of the low thermal conductivity of PCMs. However, this study also aims to show that PCM storage tanks can provide the required heating for different heat profiles of different houses.

In order to comply with the other profiles, daily heating demand is adjusted to 30 kWh but keeping the same heating profiles for three cases. Fig. 2 shows the heating loads of the three examined profiles. The heating performance of the system will be simulated if the PCM tubes

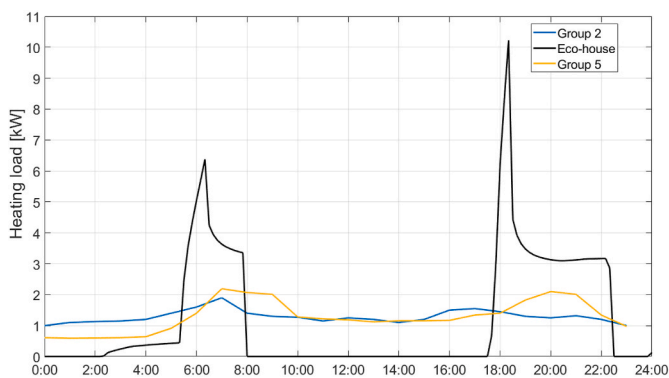


Fig. 2. Adjusted heating demands of the three cases.

can provide the required heating to the buildings in the following sections.

3. Material and method

3.1. System description

In the system, a heat pump provides hot temperature water, and the high-temperature water (70 °C) is circulated between the heat pump condenser and one of the PCM storage tanks to charge the SAT PCM tubes. When a PCM storage tank is charged, the circulating water is driven into the next PCM storage for charging it with help of the control valves. After charging, the PCM storage tanks are exposed to free cooling as they are charged for to use after days. Even after days, when heating is needed by the building, a remote-controlled triggering device activates the PCM tubes in the PCM storage tank. The PCMs inside the tubes start to crystallize immediately, and the temperature of the PCM rises to 57–58 °C. Water in the tank is heated and circulated between the house and the PCM storage tank. Relatively colder water flow comes from the building and enters the PCM storage tank, and its temperature is increased. Heated relatively high-temperature water flow directed into the building to be used for hot water and space heating requirements. Fig. 3 shows the concept of the PCM storage tanks where the heat is charged and each PCM storage tank is designed to provide one-day heating demand. Thus, the number of PCM storage tanks can be placed according to needs because this study shows the heating performance of one PCM storage tank. Since the proposed design aims to be space-effective, the PCM storage tanks can be buried under the ground. The heat storage tanks are placed in an underground container.

In this study, stored heat in the PCM tubes is partly released instead of activating the PCM tubes together. As each PCM tube is an individually enclosed unit, each tube can be activated separately. The PCM storage is designed as 14 PCM tubes inside one tank, so 14 cables will be connected to the triggering controller for each PCM storage tank. The study also aims to minimize heat losses from PCM storage to ambient during discharging period, the PCM storage tank is modelled, and the dynamic response of the storage is investigated based on different heating profiles.

3.2. PCM storage tank modelling

The PCM storage unit is designed as a cylinder container where PCM tubes are placed inside. In the simulation, the PCM storage is divided into a number of n control volumes in horizontal direction. Energy balance equations are considered in each volume. As the PCM tubes are immersed in the water, heat transfer continues during the out of heating times in discharging period. Since the PCM tubes are placed inside the tank, both latent and sensible heats comprises the storage capacity [26]. Mass transport in the tank is assumed in one dimensional and the tank length is divided into nodes and all node's energy balance equations are solved simultaneously. Additionally, each element of the tank comprises PCM tube sections, and heat transfer between the water and PCM outer surface happens. In a water element, the temperature of the water and the PCM may vary when charging and discharging take place. In order to enable heat transfer from the PCM centre to the outer edge, PCM tubes are additionally separated into radial nodes. The PCM storage tank was divided into 40 equal elements in the longitudinal direction and the PCM tubes in each element were separated by 10 radial nodes while their surrounding water is represented by one node. Fig. 4 is given to show PCM storage tank layout. 14 PCM tubes are placed inside the tank and the tank is filled with water which allows continuous heat transfer between the PCM and the water. Water element has contact with the PCM outer surface and the tank wall. Convection heat transfer happens from water to tank wall and water to PCM outer node. The PCM tube is divided into radial elements from centre to edge, thus, conduction heat transfer happens between PCM elements. The PCM storage tank

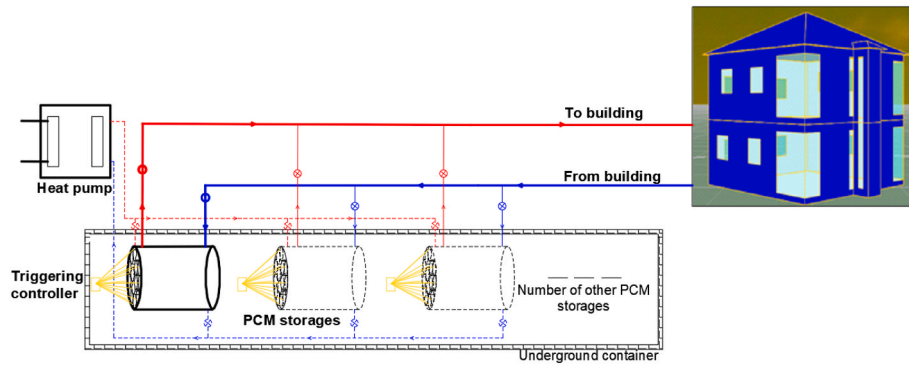


Fig. 3. Schematic of PCM storage system to provide heating.

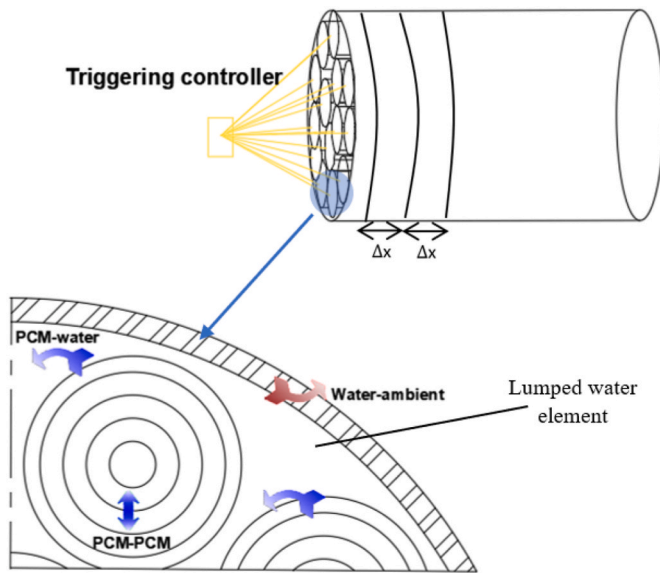


Fig. 4. PCM storage tank layout of the tank and heat transfer diagram.

calculation procedure is based on the validated previous study [10].

Generalized energy equation of the PCM is used in Eq. (1) [27,28]:

$$V_{PCMj,n} \cdot \rho_{PCMj,n} \cdot L_{PCMj,n} \cdot \frac{\partial \phi_{j,n}}{\partial t} - V_{PCMj,n} \cdot \rho_{PCMj,n} \cdot c_{p,PCMj,n} \cdot \frac{\partial T_{PCMj,n}}{\partial t} = \dot{Q}_{W_n-PCMj,n} + \dot{Q}_{PCM(j-1),n-PCMj,n} + \dot{Q}_{PCMj,n-PCMj,(n+1)} \quad (1)$$

Where j is radial node number and n indicates the number of horizontal nodes. $V_{PCMj,n}$ indicates volume, ϕ is PCM liquid fraction, $\rho_{PCMj,n}$ is density and $L_{PCMj,n}$ is the heat of fusion per unit mass of the PCM j th element at horizontal node number n . $\dot{Q}_{W_n-PCMj,n}$, $\dot{Q}_{PCM(j-1),n-PCMj,n}$ and $\dot{Q}_{PCMj,n-PCMj,(n+1)}$ are convection heat transfer rate between water and the PCM element, conduction heat transfer rate between PCM nodes in radial direction and conduction heat transfer rate between PCM nodes in horizontal direction, respectively.

Energy balance equation of the water element is given in Eq. (2):

$$T_{w,n}(i+1) = T_{w,n}(i) + \frac{\dot{Q}_{cond,n}(i) + \dot{Q}_{loss,n}(i) + \dot{Q}_{W_n-PCMj,n}(i)}{M_{St,i} \cdot c_{p,w}} \cdot \Delta t \quad (2)$$

where $\dot{Q}_{W_n-PCMj,n}(i)$ is heat transfer rate between PCM material and the water element.

Natural convection heat transfer equations for spherical shapes can be used to calculate the convection heat transfer coefficient for cylindrical shapes in the water tank [29]. Nusselt number to find natural

convection heat transfer coefficient is found by Eq. (3):

$$Nu = \left[0.825 + \frac{0.387 \cdot Ra^{1.6}}{1 + (0.492/Pr)^{9/16}} \right]^{1/4} \quad (3)$$

To calculate heat loss to the environment, Eq. (4) can be used:

$$\dot{Q}_{loss,n}(i) = U_t \cdot A_{tank,n} \cdot (T_{container} - T_{w,n}(i)) \quad (4)$$

The PCM storage tanks are assumed to be buried underground for space effectiveness, they should be placed inside a large container. The temperature of the container is assumed as 20 °C because during the day some PCM tanks are charged and some of them are discharged. $A_{tank,n}$ is heat transfer area of the water tank in one element. It is a surface area between water and the surrounding air inside the large container underground. U_t is overall tank heat loss coefficient and it is taken as 0.8 W/(m²K) [30].

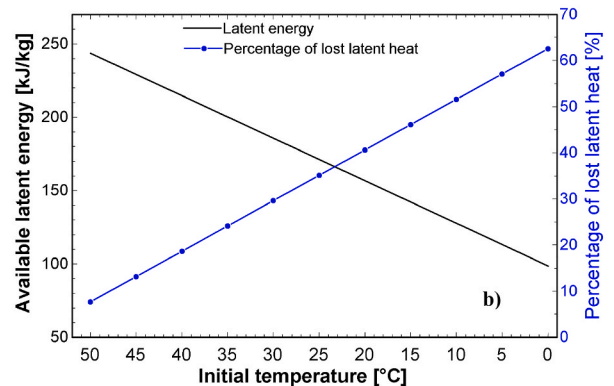
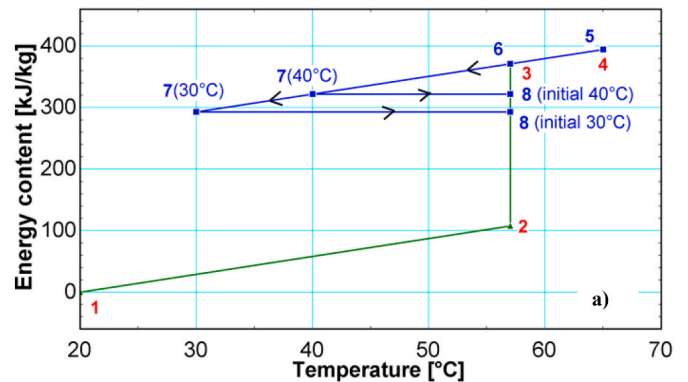


Fig. 5. a) Energy content of SAT during charging and crystallization triggering. b) Impact of subcooling degree on lost of latent heat.

Fig. 5 a is given to present the charging and discharging states of the SAT. The PCM is in the solid phase at state 1, its temperature and energy content increase by sensible heating until its temperature reaches the melting temperature at state 2. Because of the latent heat capacity of the SAT, the temperature remains constant but energy content increases until all SAT changes from solid to liquid from state 2 to state 3. State 3 to state 4 shows sensible heating of the liquid material during that period. When the charged PCM is exposed to cooling, its temperature falls from state 5 to state 6. Typically, its phase starts to change from liquid to solid at state 6, but thanks to the supercooling, the liquid phase is maintained and the PCM temperature falls to state 7. The degree of supercooling depends on cooling time or temperature difference etc. In figure 30 °C and 40 °C are given as the final temperature to show the effect of supercooling on latent heat capacity. When the PCM is triggered at state 7, its temperature increases to melting temperature immediately (state 8). However, energy content depends on initial temperature as shown in the figure because of energy conversion. Fig. 5b shows the impact of subcooling degree on energy content. As degree of subcooling increases, the latent heat capacity decreases. When the PCM temperature falls to 20 °C, the latent heat capacity of the SAT decreases by 40% which makes a serious drawback of the supercooled PCM application for long-term storage. This effect of initial temperature on performance will be investigated in the following sections.

4. Controlled crystallization and model validation

In order to test the controlled crystallization of the SAT, an electrical triggering device which includes two electrodes was prepared based on the technique described by Ref. [18]. The study offered that the electrodes can be made of various materials, however, the combination of graphite cathode (–) and a silver anode (+) was used for electric triggering of the SAT. In order to trigger crystallization, some treatments to the anodes are required, because it is necessary to have a thin layer of SAT powder on the anode surface to start nucleation. The procedure can be summarised as: The anode was polished with P80, P360 and P1200 grit sandpapers and dusted with SAT powder after each polishing, respectively. Later, to remove any remaining SAT powder on the silver rod surface, it was immersed in a 75 °C sodium acetate trihydrate solution for 2 h.

As proposed in the study, a stainless-steel tube was filled with liquid SAT at 75 °C and the prepared triggering device was placed inside the tube and also a K type thermocouple was used in the test. According to the manufacturer, the operative range is –75 °C–250 °C and the accuracy of the thermocouples is ± 0.5 °C. The top and bottom sides of the tube were sealed to avoid any leakage. The sample was exposed to free cooling for cooling down to room temperature. After being sure of the PCM temperature was 30 °C, 9 V voltage was supplied to the sample via a triggering device, and the nucleation began. Fig. 6 shows the prepared PCM tube sample and the temperature change of the SAT during the test. It can be seen that PCM temperature was increased from 29.5 °C to 57 °C

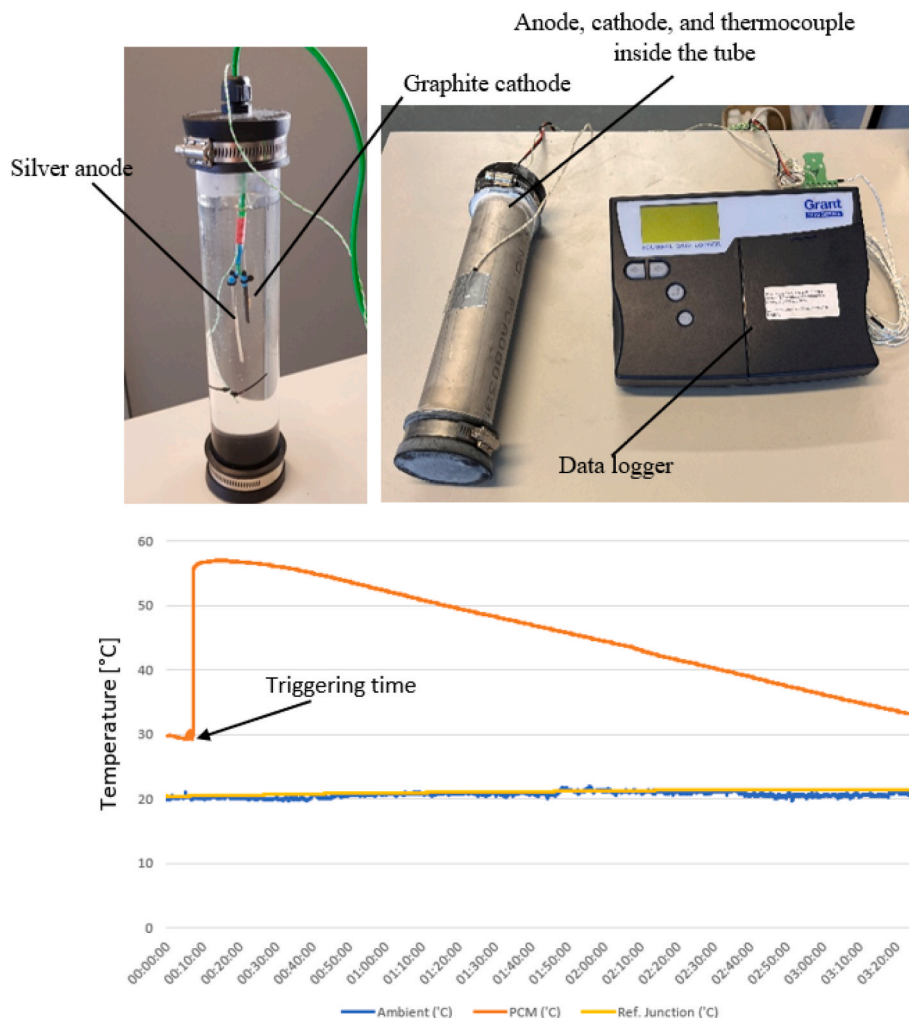


Fig. 6. PCM triggering tube sample and temperature change.

in seconds. Thus, 57 °C was used as a phase-changing temperature in the simulations. A validation study for cylindrical PCM container considering melting process, and in all tests, the errors of melting time between the model and experiment were less 5% [10].

5. Results and discussions

Since the system performance is dependent on the size and design of the PCM storage, Table 2 is given to show the design conditions of the PCM storage tank. The daily heating load was chosen as 30 kWh for three cases. Based on the validated design of the previous study, 14 PCM tubes are placed in the tank. Therefore, 14 triggering devices are connected to the controller. Half of the PCM tubes are activated at midnight which refers to starting of the simulation, and the remaining half of the tubes are activated 30 min before the morning peak load in order to prepare the temperature of the water in the tank for space heating.

5.1. Determination of initial temperature by storage time

Before simulations of heating performance, the analysis starts with testing the temperature reduction of the PCM storage after charging. It is important to see the effect of storage time because the initial temperature of the PCM when triggering occurs has an impact on the latent heat capacity of the SAT. When PCM storage is charged, the heat pump provides hot water at 70 °C, after hours, PCM crystals are melted at 57 °C and the water temperature in the tank will be at 70 °C. The tank should be used for heating just after the charging stage because of sensible heat energy in the tank can heat the house for a certain time, it shouldn't be wasted. So, the free cooling stage is assumed to start when the PCM storage temperature falls to 40 °C which is not useful for space heating. Therefore, the PCM storage tanks are exposed to free cooling during the storage time. Fig. 7 shows the temperature change of the water and PCM in the storage tank by days when the underground container temperature is 20 °C. At the end of first day, the water temperature in the PCM storage tank falls to 32.67 °C, at the end of the third day it falls to 25.4 °C. For a longer period of storage such as seven days, the tank temperature will be 21 °C which will affect the latent heat content after triggering. The impact on temperature will be investigated in following sections.

5.2. Delivery temperature variation for cases (all triggered at midnight)

In the first scenario, all PCM tubes are activated at the beginning of the day, at midnight. Although this activation is not applicable for the application of the following days, it will show the coverage potential of the heating supply of the PCM tank. The initial temperatures of water and PCMs are assumed as 30 °C. Fig. 8a shows temperature variation of the delivery and return temperature when providing heating to Group 2 buildings. At midnight, all PCM tubes are activated which means the PCM temperature increases to 57 °C immediately, and the water delivery temperature increases to around 55 °C after 30 min. Since the

Table 2
Initial design conditions of the PCM storage tank.

Daily heat demand	30 kWh	Flow rate between building and PCM storage	10 L/min
PCM tube diameter	0.09 m	Storage tank diameter	0.42 m
Total PCM mass in the tank	516 kg	Water mass in the tank	200 kg
Total PCM volume in the tank	356 L	Initial temperature	30 °C
Volume of one PCM tube	25.45 L	Tank heat loss coefficient	0.8 W/(m ² K) [30]
PCM latent heat	264 kJ/kg [17]	PCM Specific heat	2.9/3.1 kJ/(kgK) [17]
PCM conductivity	0.6/0.385 W/(mK) [17]	PCM density	1450 kg/m ³ [17]

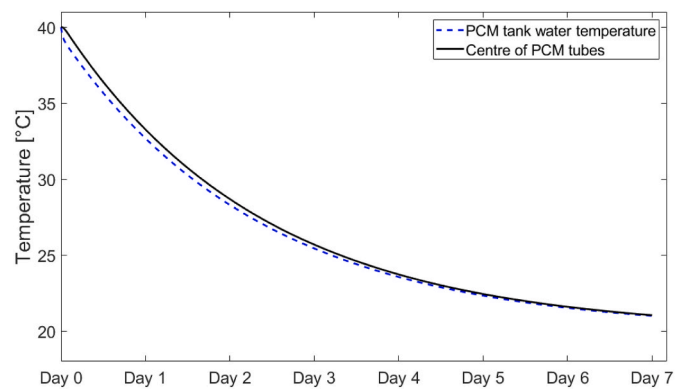


Fig. 7. Temperature change of the PCM storage during short to mid-term storage period.

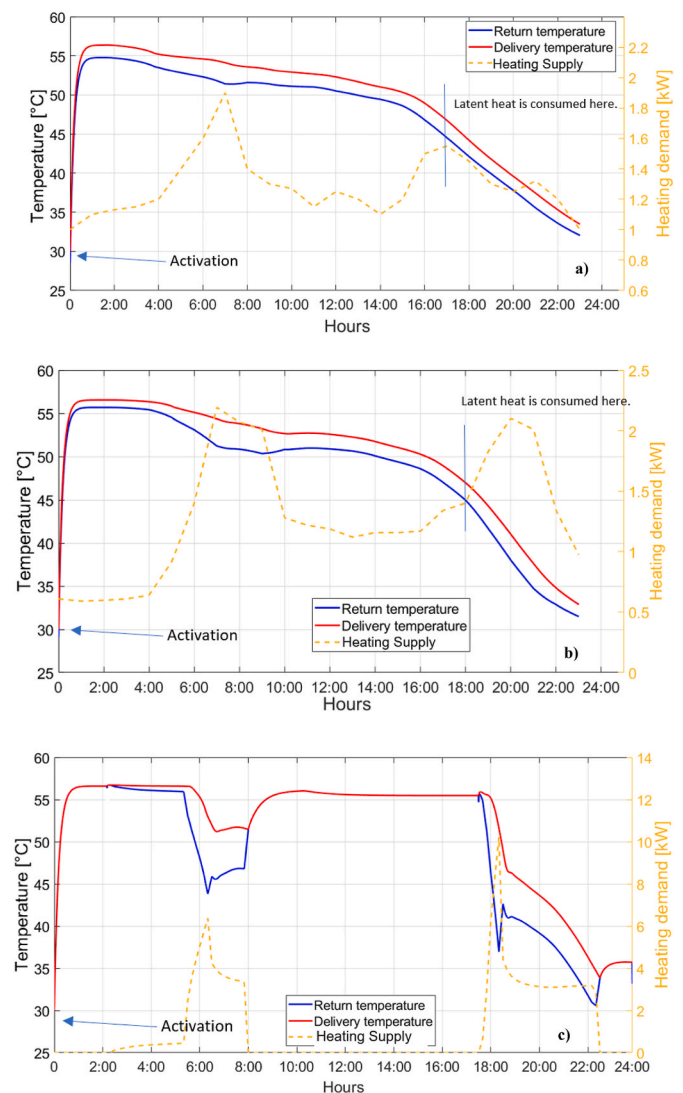


Fig. 8. Hot water supply temperature variations for Group 2 (a), Group 5(b) and Eco-house (c).

building needs heating, the water return temperature is around 2 °C lower than the delivery but the difference increases with higher heating demands during the day. The delivery temperature is 54.13 °C during the morning peak and falls to 33.45 °C at the end of the day. Fig. 8b shows the temperature variation of the supply for Group 5 buildings. A

similar activation method is followed and the delivery temperature in the morning peak is 54.35 °C and at the end of the day, 32.87 °C was observed. Fig. 8c shows the same parameters but for the Eco-house. The difference here, the morning peak occurs at 6.20 a.m. instead of 7 a.m. The delivery temperature in the morning peak is 52.97 °C and at the end of the day, the temperature falls to 35.52 °C. The delivery temperature should be higher than 40 °C in all groups and it makes it suitable for underfloor heating. However, this model is built by assuming that heating demand is extracted from the supplied water and the return temperature is calculated. It means in higher demands return temperature goes down. This approach can be okay for initial simulations but the size of the heat exchangers in the house will be constant, and the heat exchanger area should be taken into consideration in future works.

5.3. Delivery temperature variation for cases (half at midnight, half before peak)

As this study investigates different activation times of the PCM tubes, Fig. 9 is given to show the effect of different activation times on delivery temperatures. The activation time and activated number of tubes will affect temperature but here half of the PCM tubes are activated at midnight and the remaining tubes are activated 30 min before the

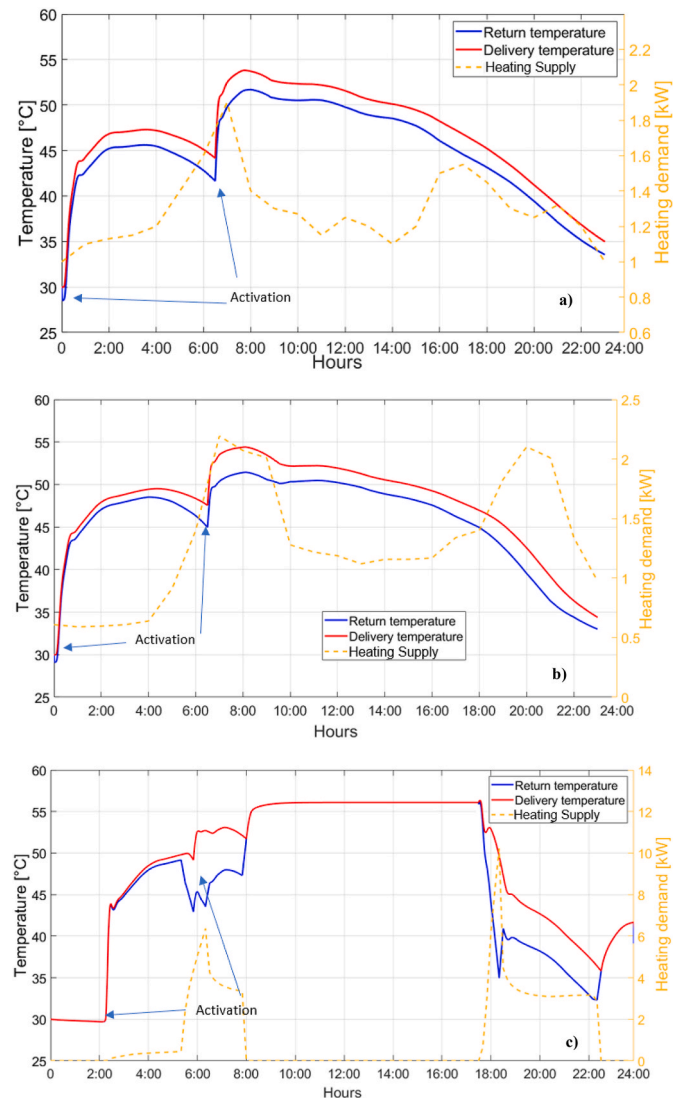


Fig. 9. Effect of different activation times on hot water supply temperature variations for Group 2 (a), Group 5 (b) and Eco-house (c).

morning peak. In order to eliminate the constant heat transfer area of the radiators, it is aimed to keep higher delivery temperatures when the demand is high. For this target, the remaining tubes are activated at 6.30 a.m. in Group 2 and Group 5, at 5.50 a.m. for Eco-house. Fig. 8a shows the delivery temperature change of Group 2.7 PCM tubes were activated at midnight and the delivery temperature reaches to maximum 47 °C because heating demand continuously consumes the activated heat and also, the remaining PCM tubes use the heat for sensible heating of tubes. After the remaining PCM tubes are triggered, the delivery temperature reaches 52.46 °C in the peak time and falls to 34.97 °C at the end of the day. In this way, the delivery temperature at the end of the day is increased by 1.5 °C by using controlled triggering. One of the reasons for this increment can be explained by the reduction of the heat losses because the daily heat loss from the SAT tank to ambient was 6.04 kWh and it decreases to 5.35 kWh by using partial triggering. Fig. 9b shows temperature variation for Group 5. After activation of half of the tubes, the delivery temperature reaches 49.6 °C because the heating load is lower than Group 2 during the early morning period. After activation of the remaining tubes, the temperature increases to 53.49 °C the peak time and falls to 34.38 °C at the end of the day. Similar to Group 2, delivery temperature is increased at the end of the day by 1.5 °C. For Eco-house, Fig. 9c is given. The first activation happens at 2 a.m. and the temperature reaches 50 °C. After activation of the remaining tubes, the temperature increases to 52.70 °C in the peak time and falls to 39.76 °C at the end of the day. Eco-house showed the highest temperature increment in the cases, delivery temperature increases from 35.52 °C to 39.76 °C by this controlling method. As expected, daily heat loss to the ambient was reduced by 1 kWh which results in a temperature rise of 4.26 °C.

5.4. Impact of initial PCM storage temperature

The effect of initial temperature on the latent heat capacity of the SAT was given in Fig. 5. The SAT may lose around 40% of latent heat when its temperature falls to 20 °C. Since the heat storage system in the proposed study aims to store heat for days, Fig. 7 was given temperature reduction rates by the day and referring to that figure, at the end of the third day the temperature falls to 25.4 °C. Thus, it is necessary to investigate the effect of the initial temperature of the PCM. Fig. 10 shows the delivery temperatures at the end of the day for examined groups considering different initial temperatures and controlling methodology. Fig. 10 also shows daily heat losses from the PCM storage during the discharging period. Overall, a higher initial temperature increases the delivery temperature at the end of the day regardless of the groups. It also increases the daily heat losses. 10 °C increase in the initial temperature results in an 8–9 °C increment in final delivery temperatures for all controlled triggering groups.

Fig. 10 also clearly shows the effect of controlled triggering on water heating performance. Controlled triggering increases the delivery temperature around 1.5 °C for Group 2 and Group 5, however, temperature increments can be achieved from 2.2 °C to 4.3 °C when controlled triggering is used in Eco-houses. Heat loss from the PCM storage varies from 0.5 kWh to 0.9 kWh for Group 2 and Group 5, but for Eco-houses, the heat loss can be eliminated up to 1.3 kWh.

6. Conclusions

In this paper, ability of the supercooled PCM storage tank to provide heating to different UK heating profiles has been investigated. Since the advantage of using SAT is the stored latent heat can be discharged externally by inducing crystallization, the heat can be stored even at ambient temperature and when it is needed. However, the effect of the initial temperature has been examined because storage time affects the latent heat capacity after activation. Moreover, controlled heat release has been adapted to different profiles to reduce heat losses from the tank. Thus, a strategy was developed to show different activation times

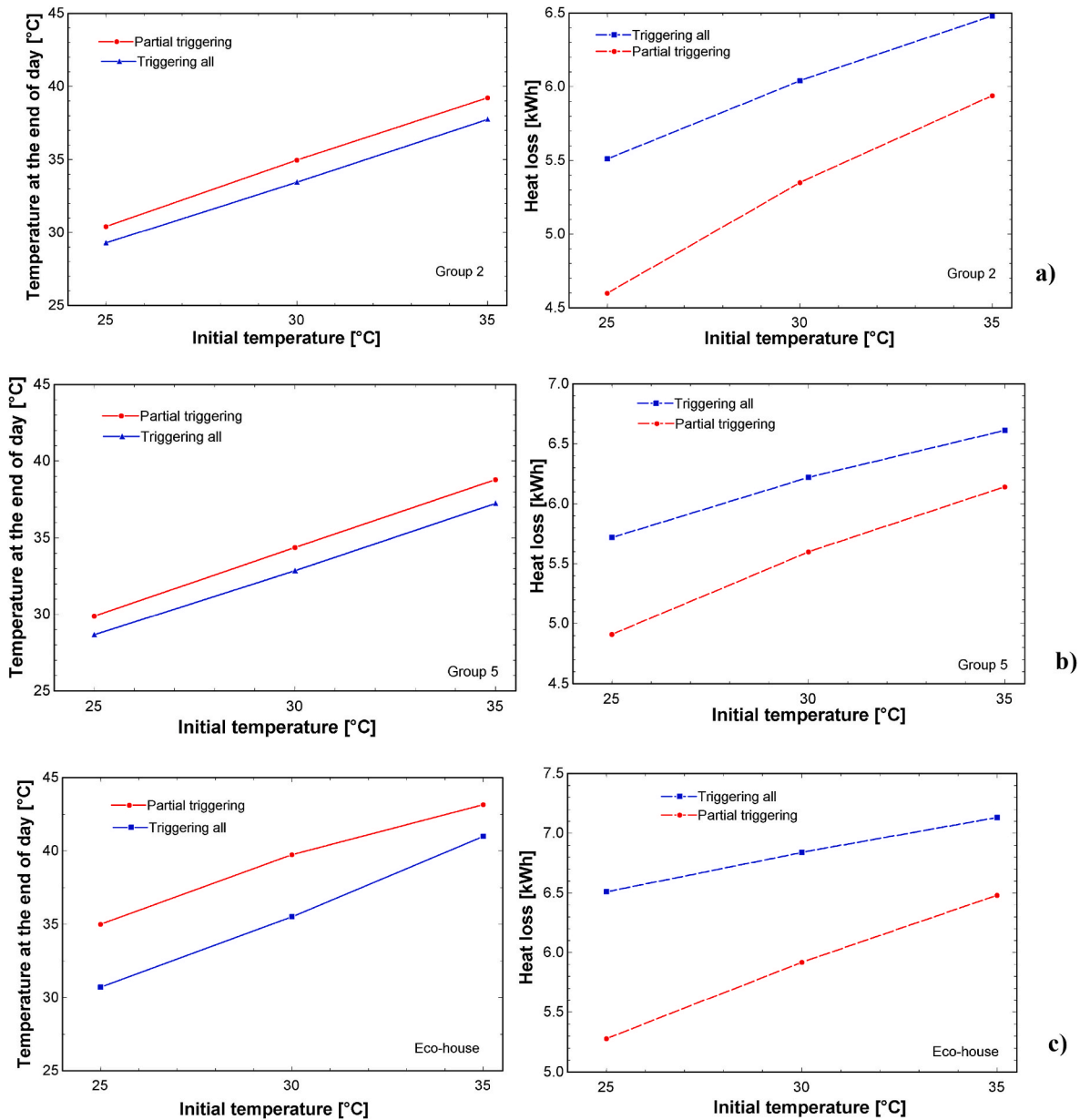


Fig. 10. Impact of initial temperature on final delivery temperature and daily heat losses, Group 2 (a), Group 5 (b) and Eco-house (c).

can give better results. This strategy shows hot water supply temperature can be increased at the end of the day and heat loss can be reduced. Based on the analysis, conclusions are drawn as follows.

- After charging PCM storage and using the sensible useful heat in the building, the stored heat can be used after three days at 57 °C but 35% of latent heat is lost.
- Controlled triggering resulted in performance improvement in all heating profiles, but it is more promising for Eco-house heating profile.
- By using controlled triggering, hot water delivery temperature is increased 1.5 °C for Group 2 and Group 5, however, 2.2 °C to 4.3 °C increment can be achieved in Eco-houses.
- Daily heat loss from PCM storage can be reduced by up to 1.3 kWh.

In future work, the number of tubes and their activation times will be optimised such as temperature-controlled activation and higher melting temperature PCMs will be used.

CRediT authorship contribution statement

Cagri Kutlu: Investigation, Software, Writing – original draft. **Yuehong Su:** Conceptualization, Investigation, Writing – review & editing. **Qinghua Lyu:** Writing – review & editing. **Saffa Riffat:** Project administration, Supervision, Funding acquisition.

Declaration of competing interest

The authors declare that they have no known competing financial interests or personal relationships that could have appeared to influence the work reported in this paper.

Data availability

The authors are unable or have chosen not to specify which data has been used.

Acknowledgements

The authors would like to acknowledge Engineering and Physical

Sciences Research Council (EP/T02318X/1) for the financial support to this research.

Nomenclature

A	Area, m^2
L	Heat of fusion, $kJ\ kg^{-1}$
M	Mass, kg
Nu	Nusselt number
P	Pressure, kPa
Pr	Prandtl number
Ra	Rayleigh number
\dot{Q}	Heat rate, W
T	Temperature, $^{\circ}C$
U	Overall heat transfer coefficient, $W\ m^{-2}K^{-1}$
V	Volume, m^3

Greek letters

ρ	Density, $kg\ m^{-3}$
φ	PCM liquid fraction

Subscripts

am	Ambient
htf	Heat transfer fluid
st	Storage
n	Node number
w	Water
t	Tank

Abbreviations

DHW	Domestic hot water
HP	Heat pump
HTF	Heat transfer fluid
IESVE	IES Virtual Environment
PCM	Phase change material
LHTES	Latent heat thermal energy storage
SAT	Sodium acetate trihydrate

References

- [1] L.F. Cabeza, M. Chàfer, Technological options and strategies towards zero energy buildings contributing to climate change mitigation: a systematic review, *Energy Build.* 219 (2020), <https://doi.org/10.1016/j.enbuild.2020.110009>.
- [2] Department for business energy and industrial strategy, UK Energy Brief in 2021 (2021) [Online]. Available: <https://www.gov.uk/government/statistics/announcements/uk-energy-in-brief-2021>.
- [3] S.O. Enibe, Thermal Analysis of a Natural Circulation Solar Air Heater with Phase Change Material Energy Storage, vol. 28, 2003, 14.
- [4] C. Kutlu, J. Li, Y. Su, G. Pei, S. Riffat, Off-design performance modelling of a solar organic Rankine cycle integrated with pressurized hot water storage unit for community level application, *Energy Convers. Manag.* 166 (15) (2018) 132–145, <https://doi.org/10.1016/j.enconman.2018.04.024>.
- [5] P. Zhang, F. Ma, X. Xiao, Thermal energy storage and retrieval characteristics of a molten-salt latent heat thermal energy storage system, *Appl. Energy* 173 (2016) 255–271, <https://doi.org/10.1016/j.apenergy.2016.04.012>.
- [6] G. Englmair, W. Kong, J. Brinkø Berg, S. Furbo, J. Fan, Demonstration of a solar combi-system utilizing stable supercooling of sodium acetate trihydrate for heat storage, *Appl. Therm. Eng.* 166 (2020), 114647, <https://doi.org/10.1016/j.applthermaleng.2019.114647>. October 2019.
- [7] J. Love, et al., The addition of heat pump electricity load profiles to GB electricity demand: evidence from a heat pump field trial, *Appl. Energy* 204 (2017) 332–342, <https://doi.org/10.1016/j.apenergy.2017.07.026>.
- [8] H.M. Teamah, M.F. Lightstone, Numerical study of the electrical load shift capability of a ground source heat pump system with phase change thermal storage, *Energy Build.* 199 (2019) 235–246, <https://doi.org/10.1016/j.enbuild.2019.06.056>.
- [9] T. Xu, E.N. Humire, J.N. Chiu, S. Sawalha, Latent heat storage integration into heat pump based heating systems for energy-efficient load shifting, *Energy Convers. Manag.* 236 (2021), 114042, <https://doi.org/10.1016/j.enconman.2021.114042>.
- [10] C. Kutlu, et al., Incorporation of controllable supercooled phase change material heat storage with a solar assisted heat pump: testing of crystallization triggering and heating demand-based modelling study, *J. Energy Storage* 55 (PD) (2022), 105744, <https://doi.org/10.1016/j.est.2022.105744>.
- [11] M. Shirinbakhsh, N. Mirkhani, B. Sajadi, A comprehensive study on the effect of hot water demand and PCM integration on the performance of SDHW system, *Sol. Energy* 159 (2018) 405–414, <https://doi.org/10.1016/j.solener.2017.11.008>. November 2017.
- [12] S. Yang, X. Shao, H. Shi, J. Luo, L. Fan, Bubble-injection-enabled significant reduction of supercooling and controllable triggering of crystallization of erythritol for medium-temperature thermal energy storage, *Sol. Energy Mater. Sol. Cells* 236 (2022), 111538, <https://doi.org/10.1016/j.solmat.2021.111538>. November 2021.
- [13] G. Englmair, C. Moser, S. Furbo, M. Dannemand, J. Fan, Design and functionality of a segmented heat-storage prototype utilizing stable supercooling of sodium acetate trihydrate in a solar heating system, *Appl. Energy* 221 (2018) 522–534, <https://doi.org/10.1016/j.apenergy.2018.03.124>. November 2017.
- [14] M. Dannemand, J. Dragsted, J. Fan, J.B. Johansen, W. Kong, S. Furbo, Experimental investigations on prototype heat storage units utilizing stable supercooling of sodium acetate trihydrate mixtures, *Appl. Energy* 169 (2016) 72–80, <https://doi.org/10.1016/j.apenergy.2016.02.038>.
- [15] G. Englmair, et al., Crystallization by local cooling of supercooled sodium acetate trihydrate composites for long-term heat storage, *Energy Build.* 180 (2018) 159–171, <https://doi.org/10.1016/j.enbuild.2018.09.035>.
- [16] G. Zhou, M. Zhu, Y. Xiang, Effect of percussion vibration on solidification of supercooled salt hydrate PCM in thermal storage unit, *Renew. Energy* 126 (2018) 537–544, <https://doi.org/10.1016/j.renene.2018.03.077>.

- [17] G. Wang, et al., Review on sodium acetate trihydrate in flexible thermal energy storages: properties, challenges and applications, *J. Energy Storage* 40 (May) (2021), 102780, <https://doi.org/10.1016/j.est.2021.102780>.
- [18] C. Dong, R. Qi, H. Yu, L. Zhang, Electrically-controlled crystallization of supercooled sodium acetate trihydrate solution, *Energy Build.* 260 (2022), 111948, <https://doi.org/10.1016/j.enbuild.2022.111948>.
- [19] W. Chen, L. Chen, L. Li, C. Dong, L. Zhang, Electrically-triggered nucleation of supercooled sodium acetate trihydrate phase change composites, *Chem. Eng. J.* 456 (2023), 141131, <https://doi.org/10.1016/j.cej.2022.141131>. December 2022.
- [20] C. Kutlu, Y. Zhang, T. Elmer, Y. Su, S. Riffat, A simulation study on performance improvement of solar assisted heat pump hot water system by novel controllable crystallization of supercooled PCMs, *Renew. Energy* 152 (2020) 601–612, <https://doi.org/10.1016/j.renene.2020.01.090>.
- [21] G. Englmair, C. Moser, H. Schranzhofer, J. Fan, S. Furbo, A solar combi-system utilizing stable supercooling of sodium acetate trihydrate for heat storage: numerical performance investigation, *Appl. Energy* 242 (2019) 1108–1120, <https://doi.org/10.1016/j.apenergy.2019.03.125>. December 2018.
- [22] R. Lowe, Department of Energy and Climate Change, Renewable Heat Premium Payment Scheme: Heat Pump Monitoring: Cleaned Data, UK Data Serv., 2017, <https://doi.org/10.5255/UKDA-SN-8151-1>, 2013-2015. [data collection].
- [23] O. Agbonaye, et al., A Clustering-Based Analysis of Heat Demand Profiles for Energy Storage and Demand Flexibility Operations, 2022.
- [24] University of Nottingham, Creative energy Homes. <https://www.nottingham.ac.uk/creative-energy-homes/houses/houses.aspx>. (Accessed 20 January 2022).
- [25] Iesve, 2020. <https://www.iesve.com/software/virtual-environment>. (Accessed 4 September 2021).
- [26] H. Huang, et al., An experimental investigation on thermal stratification characteristics with PCMs in solar water tank, *Sol. Energy* 177 (2019) 8–21, <https://doi.org/10.1016/j.solener.2018.11.004>. June 2018.
- [27] G. Manfrida, R. Secchi, K. Stańczyk, Modelling and simulation of phase change material latent heat storages applied to a solar-powered Organic Rankine Cycle, *Appl. Energy* 179 (2016) 378–388, <https://doi.org/10.1016/j.apenergy.2016.06.135>.
- [28] J. Riffat, C. Kutlu, E.T. Brito, Y. Su, S. Riffat, Performance analysis of a pv powered variable speed dc fridge integrated with pcm for weak/off-grid setting areas, *Futur. Cities Environ.* 7 (1) (2021) 1–18, <https://doi.org/10.5334/fce.121>.
- [29] R. Padovan, M. Manzan, Genetic optimization of a PCM enhanced storage tank for solar domestic hot water systems, *Sol. Energy* 103 (2014) 563–573, <https://doi.org/10.1016/j.solener.2013.12.034>.
- [30] E. Bellos, C. Tzivanidis, C. Symeou, K.A. Antonopoulos, Energetic, exergetic and financial evaluation of a solar driven absorption chiller – a dynamic approach, *Energy Convers. Manag.* 137 (2017) 34–48, <https://doi.org/10.1016/j.enconman.2017.01.041>.